FEA of CRANKSHAFT PULLEY

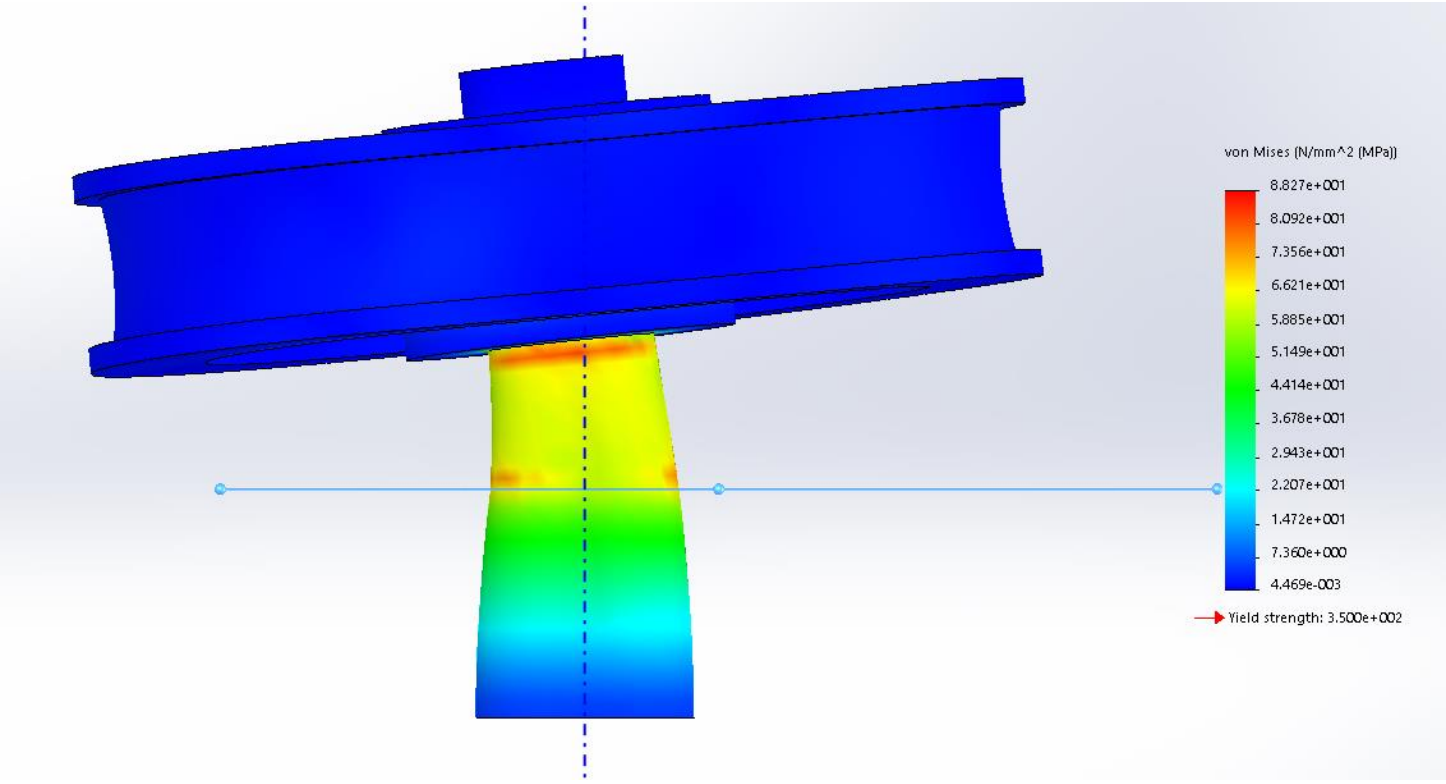

By: Yusuf Wong

Overview

For this project, I hope to increase my knowledge and understanding on how to properly conduct FEA analysis. Specifically for this project, I hope to increase my judgement of where to put boundary conditions on a model by analyzing the model's displacement and determining if they represent almost the same situation in real life. Once the model's displacement seems valid, I hope to proceed with conducting local h-refinement in order to determine convergence solutions in areas of major stress hot spots, as well as conducting sensitivity tests to further validate and justify my model's boundary conditions if time permits.

Procedure

At the beginning of this project, I was given a model representing a pulley with a shaft. The purpose of this project was to evaluate the design of this model by conducting a simulation analysis of failure when an object has penetrated one of the holes of the pulley. If the convergent, maximum, vonMises stress determined during the simulation study was higher than half the yield strength of the model, then I planned to make modifications to the design because I wanted to have a safety factor of 2.

In order to methodically evaluate the design (as well as make changes to it), I planned to first verify that the boundary conditions defined on the model during simulation studies would behave accordingly to these conditions in real life; I planned to judge the validity of the boundary conditions by assessing the displacements of the model after running the simulation. After verifying the boundary conditions, I then planned on proceeding with stress analysis on the model of study. If the maximum, convergent value for stress was higher than half the yield stress of the material, then I planned to make modifications to the model, create a new study, and then repeat stress analysis of the new study.

Testing Suggested Initial Boundary Conditions of the Original Model (Experiment 1):

For my first boundary conditions experiment (Experiment 1), I was suggested to try restraining a face on one of the holes of the pulley and applying a torque of 100 N-m (whose direction is along Axis1) on the outer surface of the larger part of the shaft that is pushing against the restrained surface, as shown in the following figure:

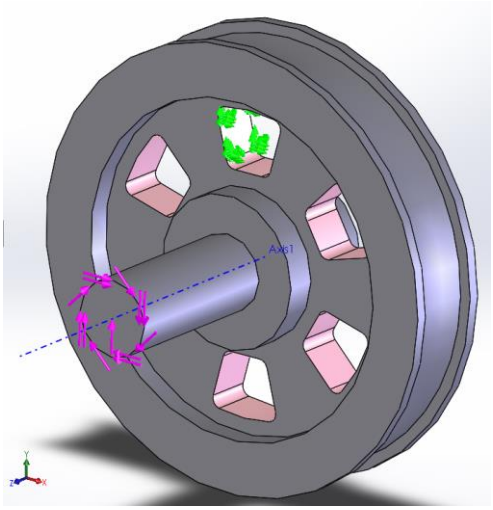

Figure 1: Applying Boundary Conditions for Experiment 1

After applying a mesh with global elements of size 5.00 mm, I ran the study to get results for values of stress and displacements of the model. I used the "Deformed Result" feature in order to analyze if the displacements of the model seem valid. Figure 9 shows the initial, undeformed view, and Figure 10 shows the deformed view after applying torque on the shaft of the model. I intentionally left Axis1, which represents the axis for radial symmetry of the original model, in both figures in order to show a comparison.

After conducting this experiment, I saw that after running the simulation, the entire model translated in an abnormal way. By comparing the top views before and after deformation, the model translated in the x-direction, since Axis1 is the axially symmetric axis of the original mode. Figure 10 shows that the entire "deformed result" translated away from the symmetric axis. This should not happen because even the front face where torque was applied also translated; this is represented in Figure 10 where the bottom edge (which represents the face) is not symmetrical about Axis1. This should not occur in a real-life scenario because a portion of the shaft should be connected to a motor. If we assume that the motor is rigid and does not move, then the face of applied torque should not move either. However, this experiment does not represent this scenario. Thus, from this experiment, I knew that these initial boundary conditions were invalid. I also realized how important it was to make sure that the boundary conditions represent the real-life situation as closely as possible.

Re-assessing Boundary Conditions by Looking at Real Pulleys:

Instead of just randomly putting boundary conditions on SolidWorks and hoping to find a valid simulation study that can represent a real-life scenario of what would happen when one of the holes of the pulley was accidentally obstructed by a rogue object, I began to look at motorized pulley-and-shaft systems and understand how they operate first instead:

Figure 2: Motorized Shaft-Pulley Mechanism from a 3D Printer

The photo in Figure 2 shows a shaft connected to a motor. Attached on the shaft was a pulley with a belt wrapped around it. I turned the shaft to see how the shaft and the pulley operates. I saw that the shaft was able to rotate about its center axis. I also realized that the shaft was able to freely rotate within the hub of the motor; because the shaft was not allowed to translate outside of the motor, I realized that only part of the shaft had to be lodged inside the motor to prevent it from translating. Consequently, I realized that part of the shaft lodged inside the hub of the motor had to behave like a fixed hinge that can rotate about its center axis, but not translate in any other direction. However, any other part of the shaft NOT inside the hub of the motor did not have any restraints on it.

I then looked at the pulley and the belt assembly. The section on the cylindrical surface of the pulley where the belt touches and wraps around the pulley seems to restrain the pulley from translating; when the motor is turned on and the shaft rotates, the tension of the belt connected to the pulley allows the pulley to move the belt when the motor applies torque to the shaft. As a result, it appears that the tension of the belt could prevent the pulley from translating.

However, I think this would really depend on the type of the belt being used within the mechanism of the assembly. Thus, if the belt's material is made from a weaker material, such as rubber, with a much smaller Young's Modulus than that out of the material of the pulley and a force is applied to the pulley to bend about its central axis, then the effect of the belt preventing translational motion is nominal. In other words, if the belt is made from very weak material, then I believe that the belt would not really restrain the pulley from translating in any direction. (Nonetheless, if the material of the belt has a very high yield strength, such as a very strong steel cable, then I would change my assumption about the possibility of free translational motion of the pulley.) Thus, for the rest of my studies, I planned to not make the assumption that the belt will prevent translational motion of the pulley by assuming that the material used for the belt is made from a much weaker material than steel.

After analyzing the type of restraints on a general, motorized shaft-pulley mechanism, I began a static analysis on what would happen if one of the faces from one of the holes in the pulley of the original model was restrained by an obstacle preventing the pulley's rotation. The following figure on the next page will help summarize my analysis and predictions:

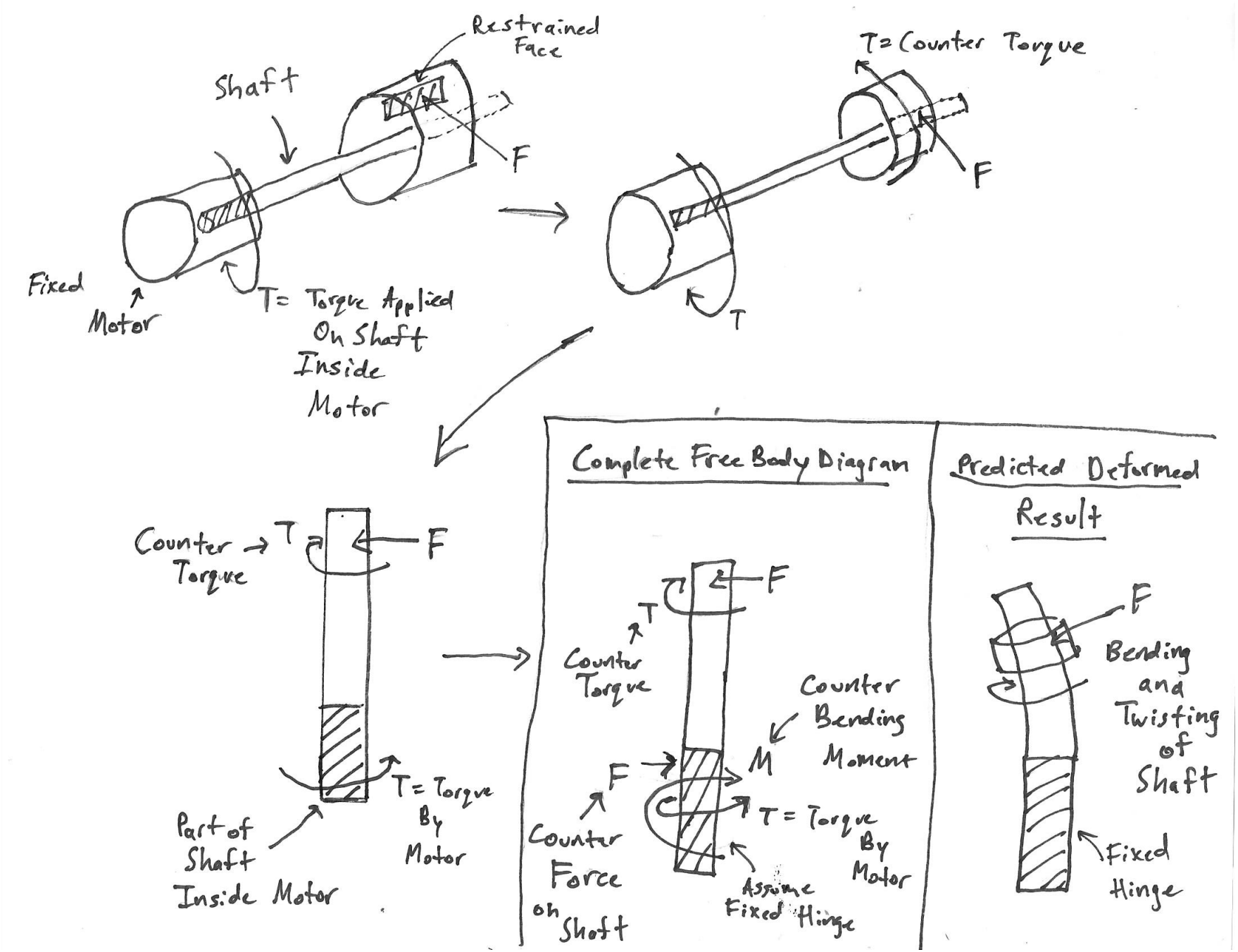

Figure 3: Prediction Using Hand-Drawn Static Analysis

The previous figure shows that a portion of the shaft is located inside the hub of the motor. This part of the shaft would have a hinge restraint that would prevent this portion from translating if we assume that the entire motor is restrained. As a result, this part of the shaft would only be free to rotate about its central axis. Additionally, if the face of the hole in the pulley is restrained, then this is almost the same thing as saying that a force is being applied on this face. This force is applied by a distance away from the central axis of the shaft; this is analogous to having force being applied to the center of the shaft and having a torque applied about the axis of the shaft, which gets canceled out by the torque applied by the motor in order for the sum of the torques to equal to 0. For this scenario to be completely static, however, a counter-force had to be applied to the part of the shaft lodged inside the motor. Consequently, a moment was created by the two forces shown in the free body diagram. As a result, a counter-bending moment (shown as "M" in the previous figure) also had to be applied to this part of the shaft as well.

Thus, the part of the shaft lodged inside the motor had to behave somewhat like a fixed support to counter the forces and torques created when a face on the pulley is retrained. As a result, I knew that for the simulation study, this part of the shaft had to be a fixed hinge, since it does not translate in any direction. Additionally, the fixed hinge would only be allowed to rotate about its central axis. As a result, the counter bending moment and counter force would not allow this part of the shaft to rotate or translate in any other direction only if I make this part of the shaft a fixed hinge. Thus, after creating the free body diagram, I then tried to predict how this mechanism would deform. By analyzing the types of restraints, I predicted that part of the shaft and the pulley would twist about its original axis of rotation, as well as bend at an angle away from its central axis of rotation, as shown in the previous figure.

Applying New Set of Boundary Conditions on SolidWorks (Experiment 2):

After analyzing on how a motorized shaft-pulley mechanism could work, I began to make a simulation study on SolidWorks. I first started by first modifying the model by creating a split line on the longer end of the shaft. I did this by first creating a parallel plane offset by 35.00 mm from the face where the torque will be applied, as shown in the following figure:

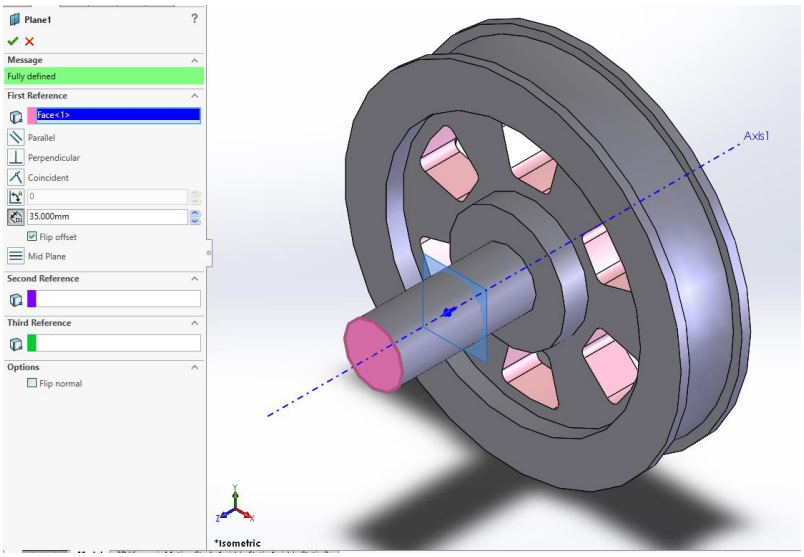

Figure 4: Offsetting Parallel Plane from Front Surface of Shaft

I then used the split line feature to split the outer face of the shaft into two different surfaces that I can distinguish during the simulation study:

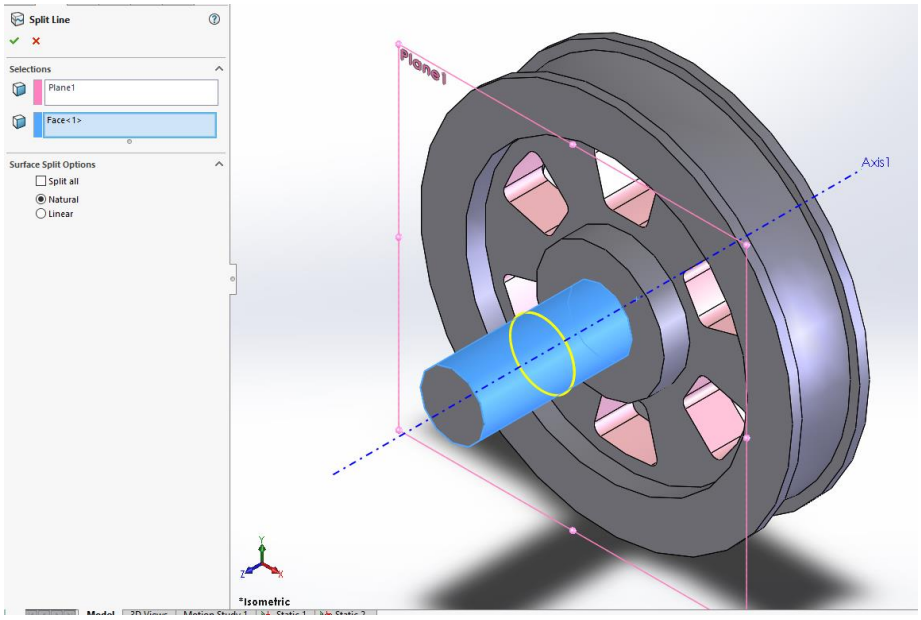

Figure 5: Creating Split Line to Split the Shaft into 2 Sections

I kept the same fixed restraint on one of the surfaces of the holes as the previous experiment (as shown in Figure 1). However, I decided to change the way torque is applied, as shown in the following figure:

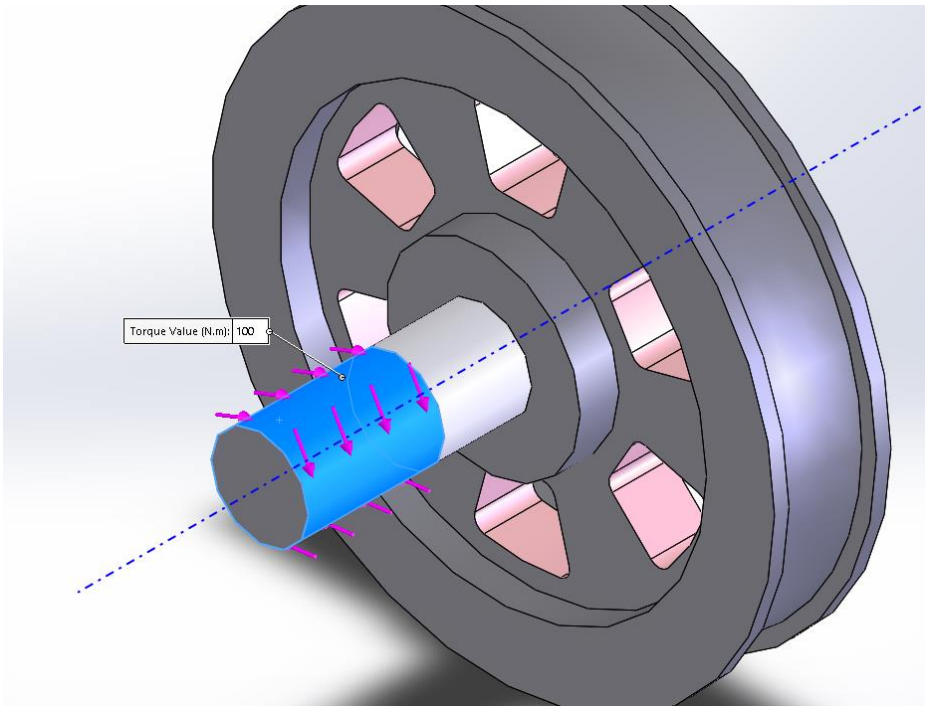

Figure 6: Applying Torque on Entire Cylindrical Surface for a Section on the Shaft

I decided that this change was necessary because this part of the shaft is located inside the hub motor. Consequently, I assumed that this entire portion of this shaft will be rotated by the motor and create a torque on the entire surface, since I wanted to replicate this type of boundary condition in real life. It did not make sense to me that a torque was applied about the front surface of the shaft; rather, it made more sense that torque was applied around a section of the cylindrical face of the shaft. However, I know that this may or may not be the case in real-life because it would depend on how the motor provides torque on the shaft. Nonetheless, for this study, I decided to arbitrarily choose the 35.00 mm portion of the shaft that will be subjected to a torque of 100 N-m.

Additionally, I added a fixed hinge restraint for this part of the shaft as well, since it would be located inside the motor and only be free to rotate, but not translate in any other direction. This can be shown in the following figure:

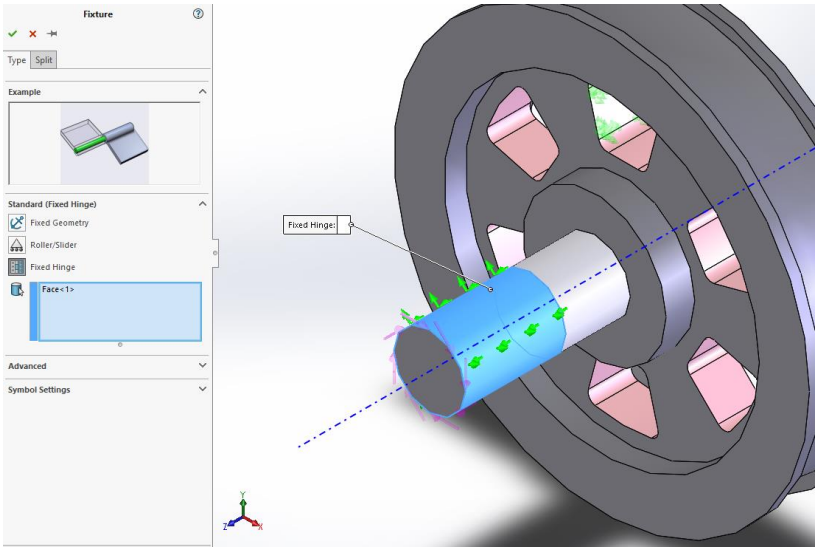

Figure 7: Applying Fixed Hinge Restraint for a Section on the Shaft

I then created a mesh with 2nd order, global elements of size 4.00 mm and then ran the simulation.

After running the simulation, I believe my prediction for the deformed result shown in the top and side views of the model shown in Figure 12 and Figure 14, respectively, was correct after comparing from them from their original views. From Figure 12, I saw that the fixed hinge part of the shaft was axially symmetric about Axis1 and that the rest of the model gradually bended about an angle away from the central axis.

However, looking at the deformed result, it appears that the radius of the hinged portion of the shaft increased when comparing it to the undeformed result. This should not have happened because I defined this portion of the shaft to be a fixed hinge, which should have prevented the radius of this portion of the shaft from changing in magnitude. I then investigated this issue by looking at the magnitude and direction of displacement in vectorized form in two different ways: as a deformed and undeform result. As shown in Figure 16, I selected the "Deformed Result" option, as shown in the red arrow on the top of the figure. By selecting this feature, SolidWorks showed that the direction of displacement of these vectors were in the radial and tangential direction. However, in Figure 16, I unselected this option when displaying these vectors, and the figure shows that the vectors are only displacing tangentially, not radially. In fact, for every cross-section of the hinged portion of the shaft, each displacement vector is tangential to the outer surface of the shaft. This is what should have happened when a fixed hinge is applied this portion of the shaft, since a fixed hinge can only displace in the tangential

direction. Thus, I believe that SolidWorks created a graphical anomaly when trying to show displacement in the hinged portion of the shaft when using the "Deformed Result" feature, which might have occurred because a torque was applied on the same surface as the hinge and gave a weird and deformed visual result. Additionally, I realized that vector plots should be used when the "Deformed Result" feature is turned off in order to more accurately display displacement results.

However, I do believe that the deformed result shown in Figure 12 correctly displayed how the pulley would deform after analyzing its displacement vector plot (as an undeformed result). As shown in Figure 17, the vectors on the left side of the shaft is pointing away from the axis and downwards, while the right side of the shaft is pointing towards the axis and upwards. This is similar to how the deformed result of the pulley looks like in Figure 12.

After analyzing the displacement results, I decided that my boundary conditions, including how torque should be applied on the shaft, were accurate enough to simulate what could actually happen in real-life. However, this decision was a double-edged sword because this simulation of boundary conditions created several stress singularities.

Analyzing Stress Hot Spots of Experiment 2:

After running the simulation, I saw 4 locations of stress hot spots that I felt were important to investigate, which can be shown in Figure 18. The following will summarize their respective locations by the numbers from the figure:

1) Circular Edge Interface between Hinged and Unhinged Sections of the Shaft
2) Shaft-Disk Interface
3) Disk-Pulley Interface
4) Edge on Fixed, Rectangular Face

I explored each of these possible, high stress concentrations by conducting local h-refinement for each location individually with a constant global element size of 4.00 mm. I then used probing to determine the maximum stress within each region. The summary of my results for h-refinement at locations 1, 2, 3, and 4 can be shown in Table 1, Table 2, Table 3, and Table 4, respectively.

The data in Table 1 shows that the value for stress at the circular edge interface between the hinged and unhinged sections of the shaft diverges as I iterated decreasing values of local element size. Initially, I was afraid that I created a stress concentration factor at this section of the shaft by using the boundary conditions that I had chosen for this experiment. However, I

realized this stress singularity occurs at the end of the fixed hinge boundary condition. Because torque was applied at the hinged portion of the shaft against the fixed restraint from one of the faces of the holes in the pulley, a bending moment of the unhinged portion of the shaft occurred (which can be seen again in Figure 12) about the hinged portion of the shaft, since the hinged section had zero degrees of translational freedom. In fact, the hinged section behaved almost like a fixed support, but with only had 1 degree of rotational freedom. As a result, the shaft bended at an angle and created a sharp turn in geometry between the hinged and unhinged sections of the shaft. If this is not convincing, then imagine the shaft as a line segment broken into two halves. If one of the halves is restrained and the other half was to rotate in order to bend, then a sharp corner is created at the point where the two halves meet. Thus, the software was trying to determine a value for stress at a sharp turn in geometry. A stress singularity developed because as the local elements of refinement became smaller, the stress at this sharp turn increases indefinitely. Thus, it made sense a stress singularity should occur at this interface, and I believe that not much can be done to fix this stress singularity at the edge of a fixed hinged boundary condition and that stress in this location should be ignored.

Stress singularities also occurred at both the shaft-disk and disk-wheel interface, which can be shown in regions 2 and 3 (respectively) in Figure 18, after conducting local h-refinement at both regions (which can be shown in Table 2 and Table 3). I expected this to occur because there were sharp changes in geometry at both interfaces. Additionally, I noticed that after conducting local h-refinement at both interfaces, the shaft-disk interface had relatively higher values of stress than those of the disk-wheel interface, despite that the values for stress for both locations diverge. In other words, the rate at which stress diverges for the shaft-disk interface seems higher than that of the disk-wheel interface. Nonetheless, I believed that it would be safer to add fillets at both locations to remove these stress singularities. However, instead of creating two fillets on the model, I also thought it would be wiser to create only one fillet that connects the shaft directly to the wheel (just like killing two birds with one stone) and create only 1 stress concentration factor instead of two. I then planned to conduct stress analysis at this location to make sure it was below cold rolled steel's yield stress of 350 MPa at a safety factor of 2, which basically meant that the maximum value for stress should be lower than 175 MPa.

Finally, I saw that a stress singularity also developed near the fixed, rectangular region where the object was supposed to restrain the pulley from turning. By conducing local h-

refinement in this region and probing for the maximum stress for every iteration of decreasing local element size, the stress in this region kept increasing. In fact, the value for maximum stress kept increasing on one of the edges of the fixed, rectangular boundary condition. However, this problem may or may not still be prevalent after I modify the model's geometry and add a fillet between the shaft and the wheel. Thus, if this problem still exists after adding filleted geometry and conducting stress analysis, I will discuss further about the stress singularity (if there still exists one).

Modifying the Model's Geometry (Experiment 3):

Learning from the previous experiment, I decided to add a fillet that directly connects the shaft and the wheel by modifying the original sketch, which can be shown in the following figure:

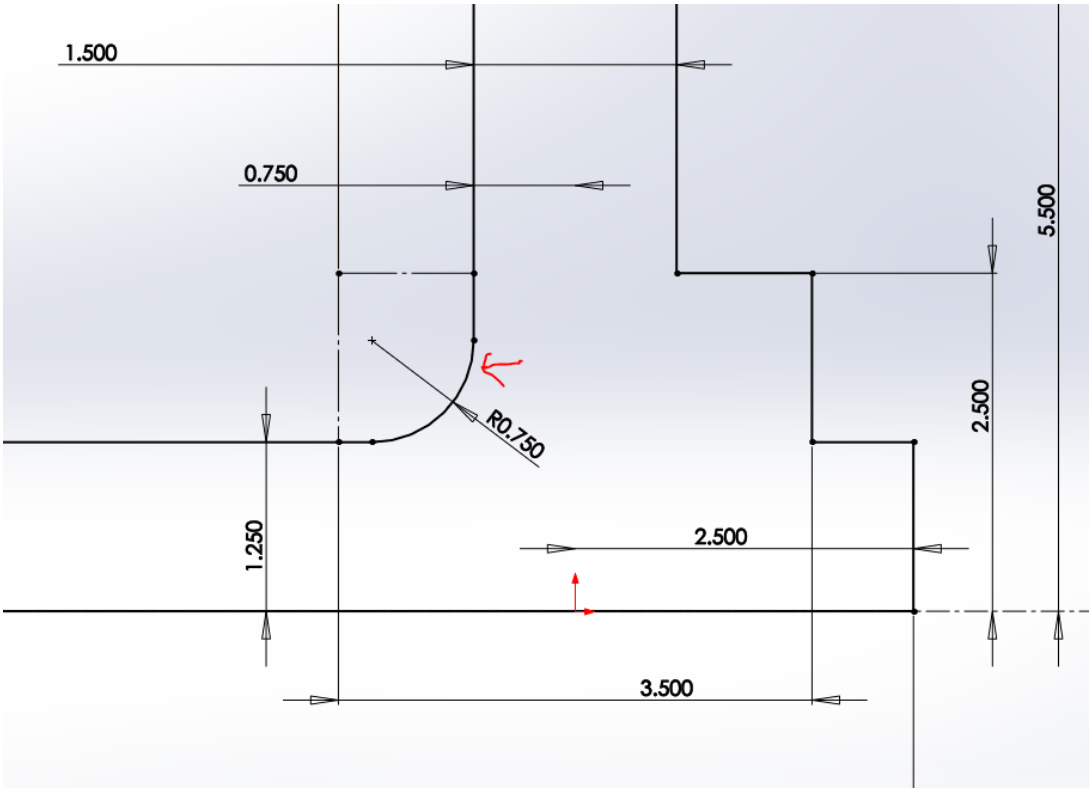

Figure 8: Adding Fillet between Shaft and Wheel

I added a 0.75 mm fillet to the original sketch. After the model was scaled by a factor of 10, the actual size of the fillet that I created was 7.5 mm. I then created a study with the same boundary conditions as the previous experiment and used 2nd order global elements of 4.00 mm. The distribution of the stress, as well as locations of stress hot spots, can be shown in Figure 19.

Analyzing Modified Model's Stress Hot Spots:

After modifying the model's geometry, Figure 19 still showed stress concentration at the interface between the hinged and unhinged portion of the shaft and at the fixed, rectangular surface. The previous experiment showed that the stress concentration at the hinged and unhinged interface should be ignored because a stress singularity developed at the edge of the boundary condition. Because I did not modify the same boundary condition for this experiment, the stress concentration at this location can also be ignored.

Just like in Experiment 2, the results of Experiment 3 still showed that a stress singularity developed on the edge of the fixed rectangular surface. Because I saw that a fillet was connected to the edge of the rectangular surface, I originally thought that the stress would evenly be distributed. However, the results from this experiment showed that the value for stress at the interface between the fixed rectangular surface and the filleted surface diverges at local h-refinement was applied. By taking a closer look at the mesh at an iteration of local refinement, which can be shown in Figure 20, I saw that most of the elements on the fixed surface had very nominal values for stress (between 10-15 MPa). However, the stress drastically increased as the elements approach to the boundaries of the fixed surface. In fact, at one of the edges of the fixed rectangular surface, the stress in this location spiked to approximately 482 MPa. After pondering about why this might be the case, I realized that the elements on either side of the interface would always be connected by a sharp turn in geometry, as shown Figure 21. This was true even by having a fillet connected at the interface, since the software was limited in trying to create curved geometry during this experiment. As a result, SolidWorks was trying to determine stress at a sharp edge in geometry, and it made sense that the value for stress increases for every iteration of smaller, local element size. Thus, I believe that the stress in this location of discontinuity can be ignored for this analysis.

Finally, high stress concentration developed on the fillet connecting the shaft and the wheel. After conducting local h-refinement with decreasing local element size and probing for maximum stress, however, I was finally able to get a convergent value of 76 MPa for stress at this location, which can be shown in the data on the graph of Figure 22.

Results

EXPERIMENT 1 RESULTS:

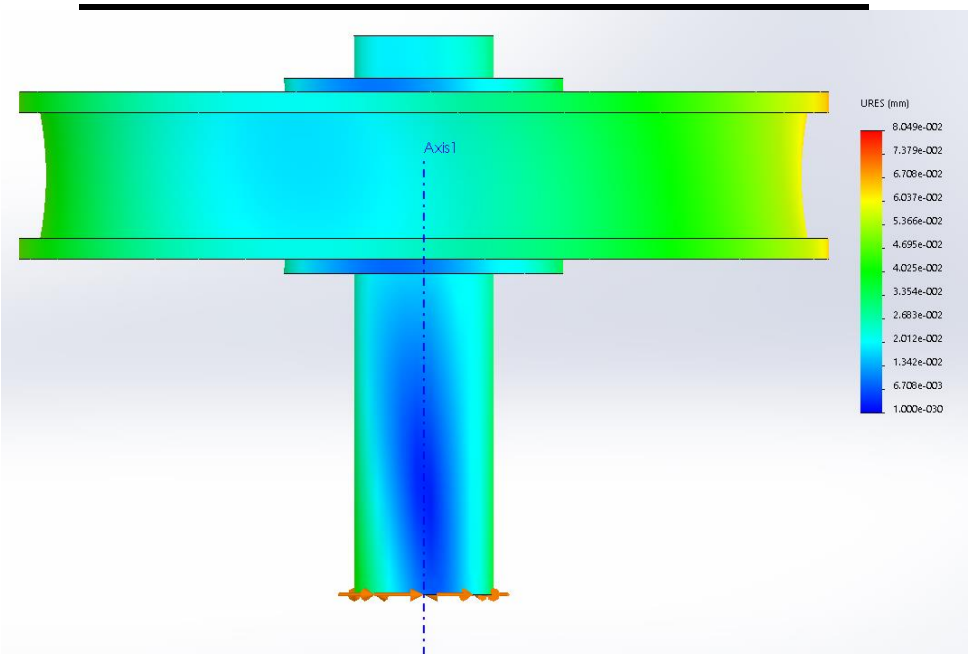

Figure 9: Undeformed Top View of Experiment 1

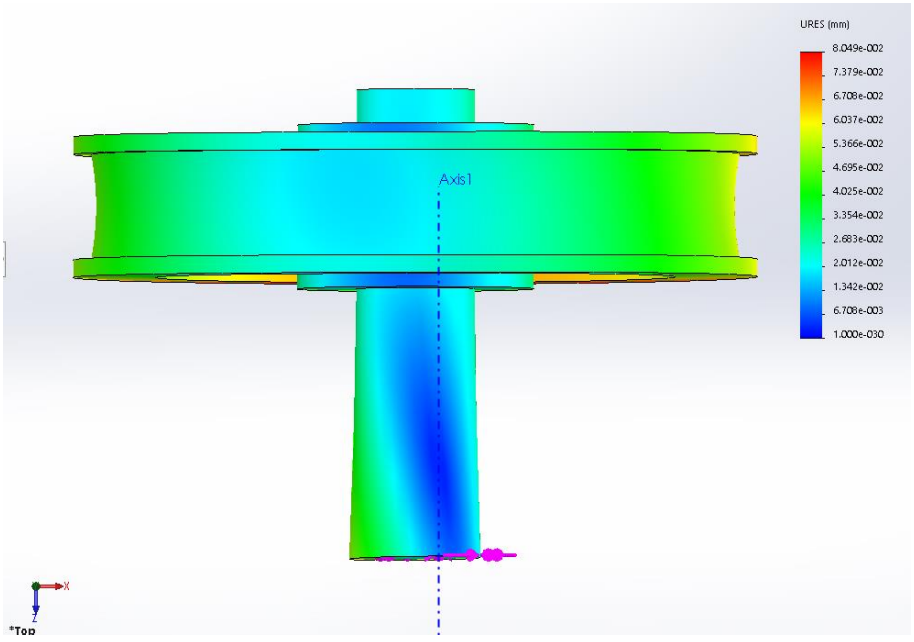

Figure 10: Deformed Top View of Experiment 1

EXPERIMENT 2 RESULTS:

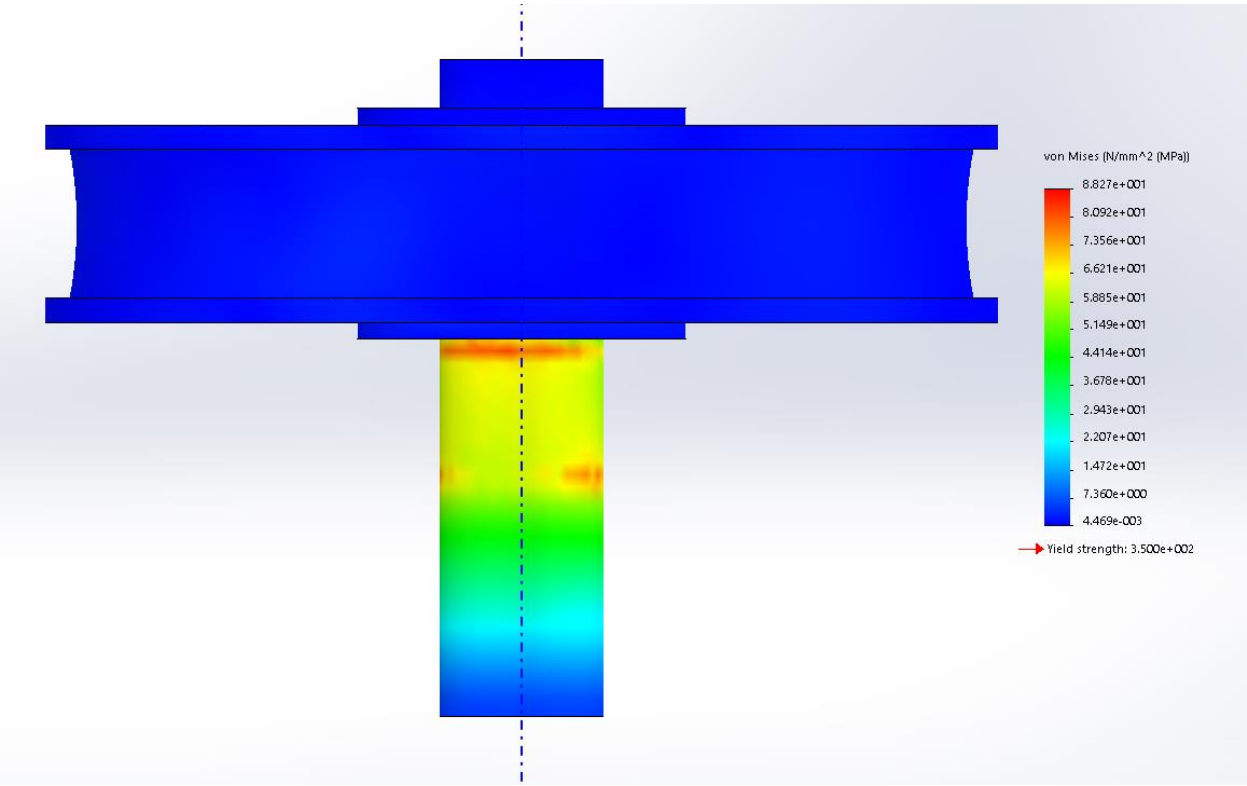

Figure 11: Undeformed Top View of Experiment 2

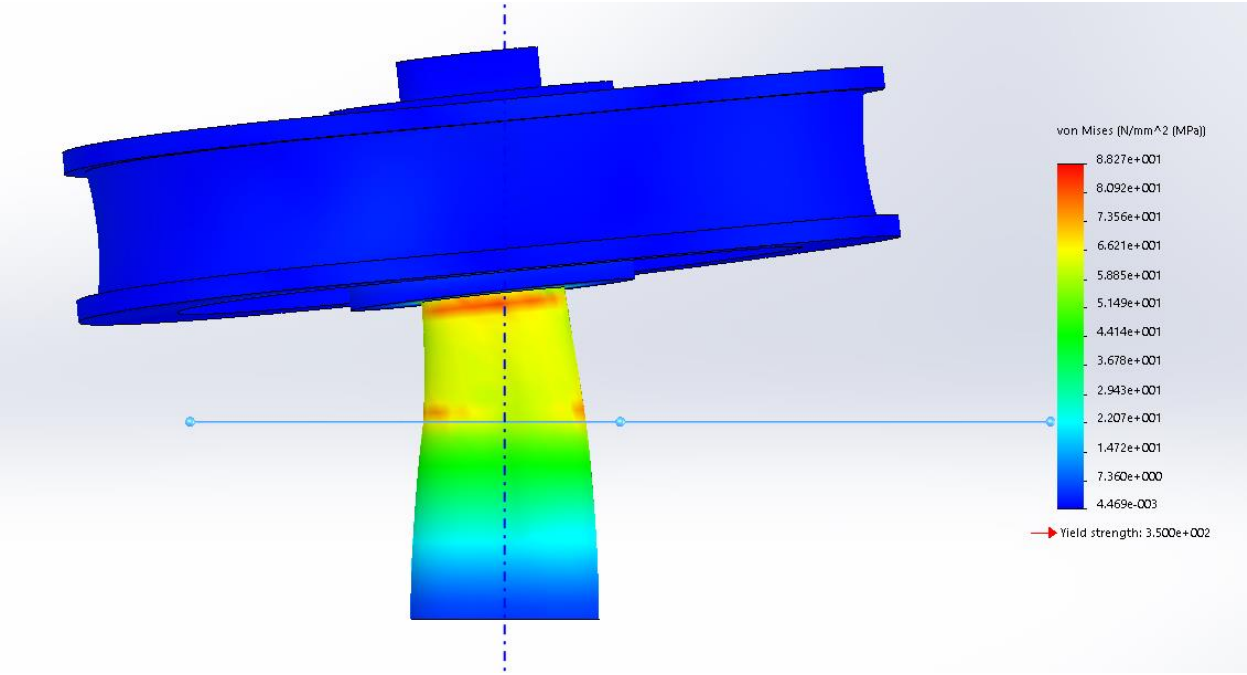

Figure 12: Deformed Top View of Experiment 2

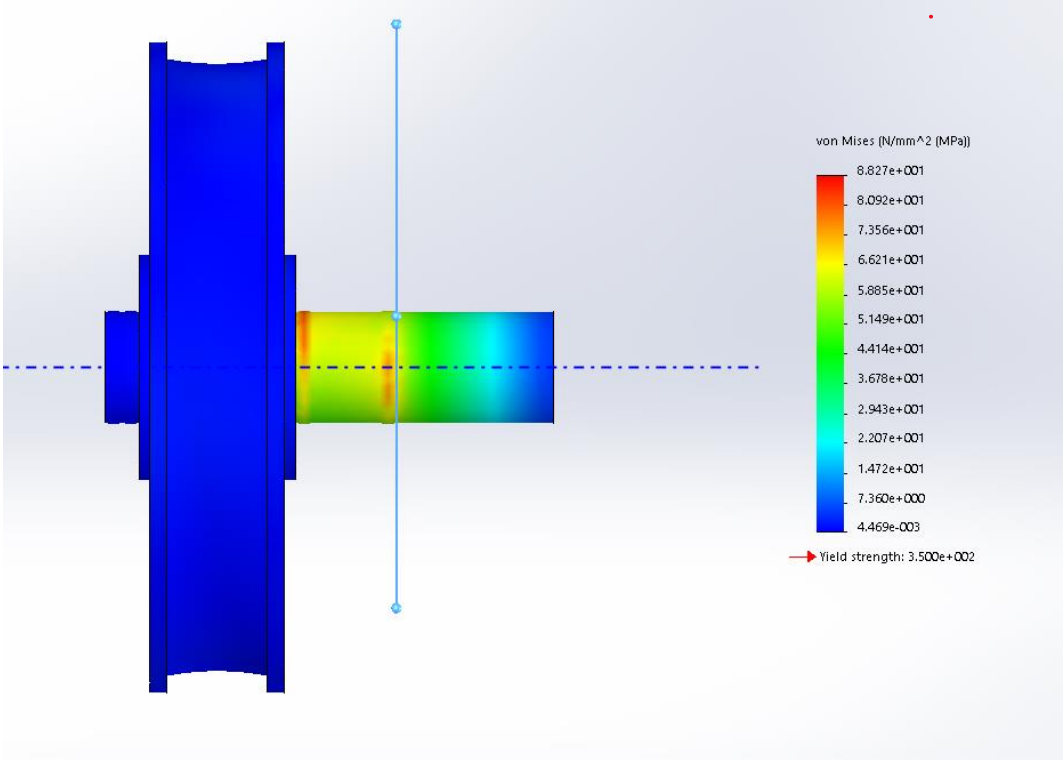

Figure 13: Undeformed Side View of Experiment 2

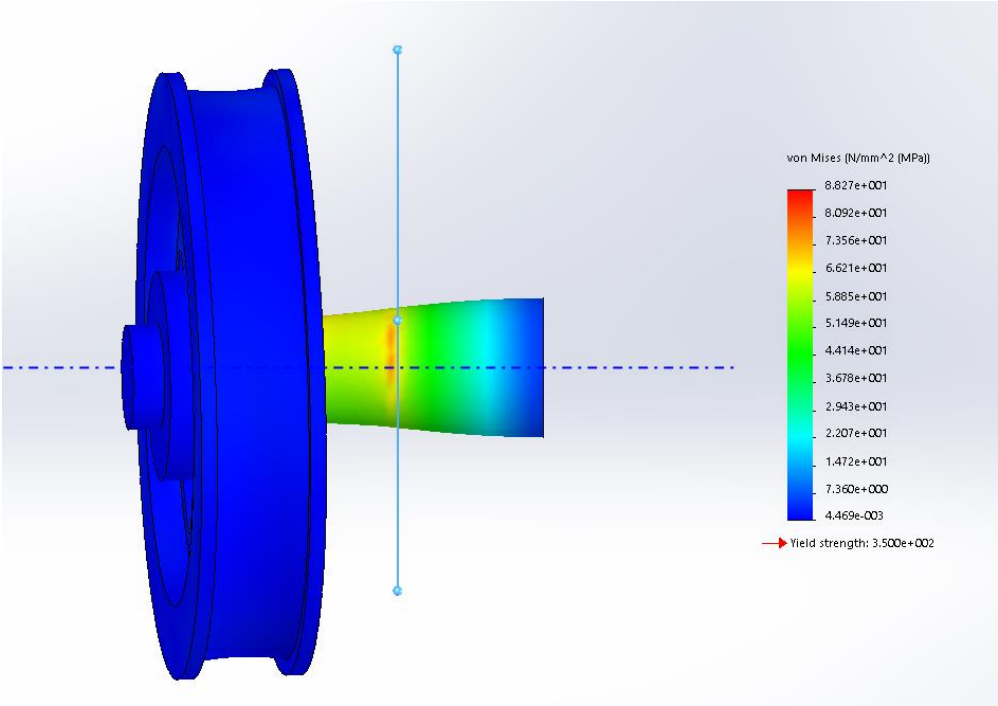

Figure 14: Deformed Side View of Experiment 2

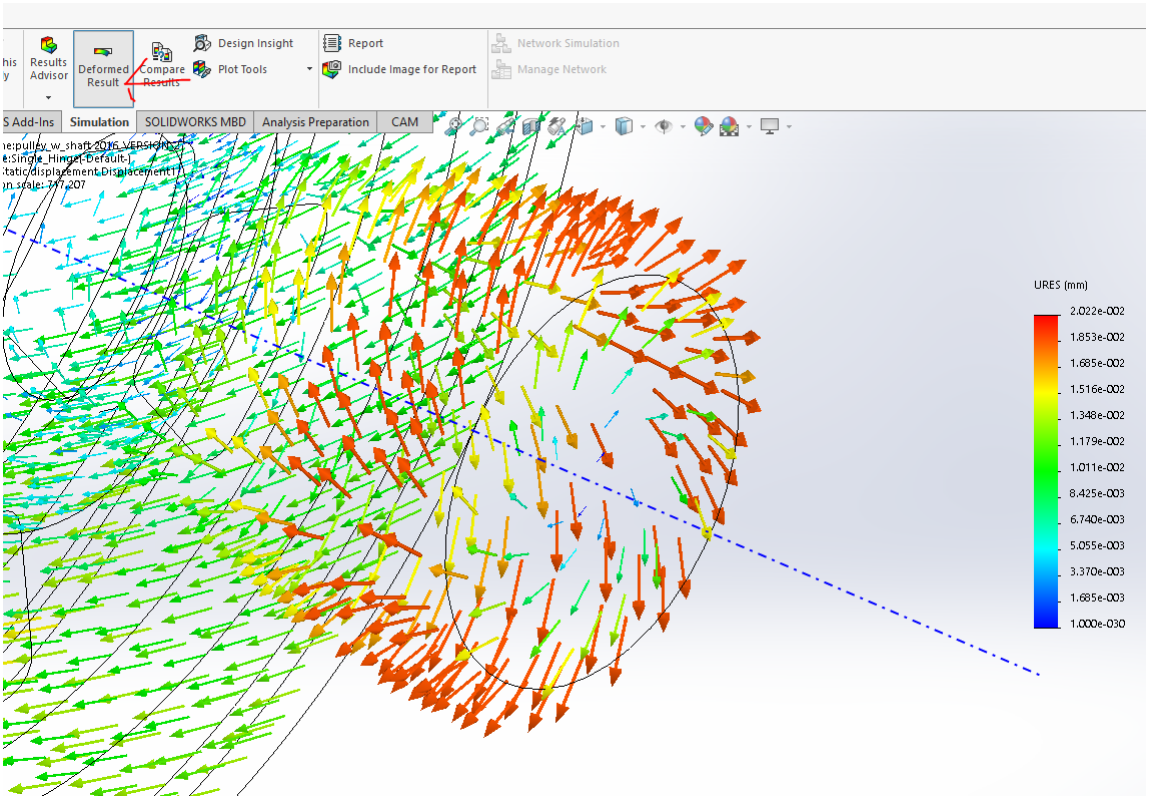

Figure 15: Showing Displacement (As Deformed Result) Vector Plot of Hinged Portion of Shaft

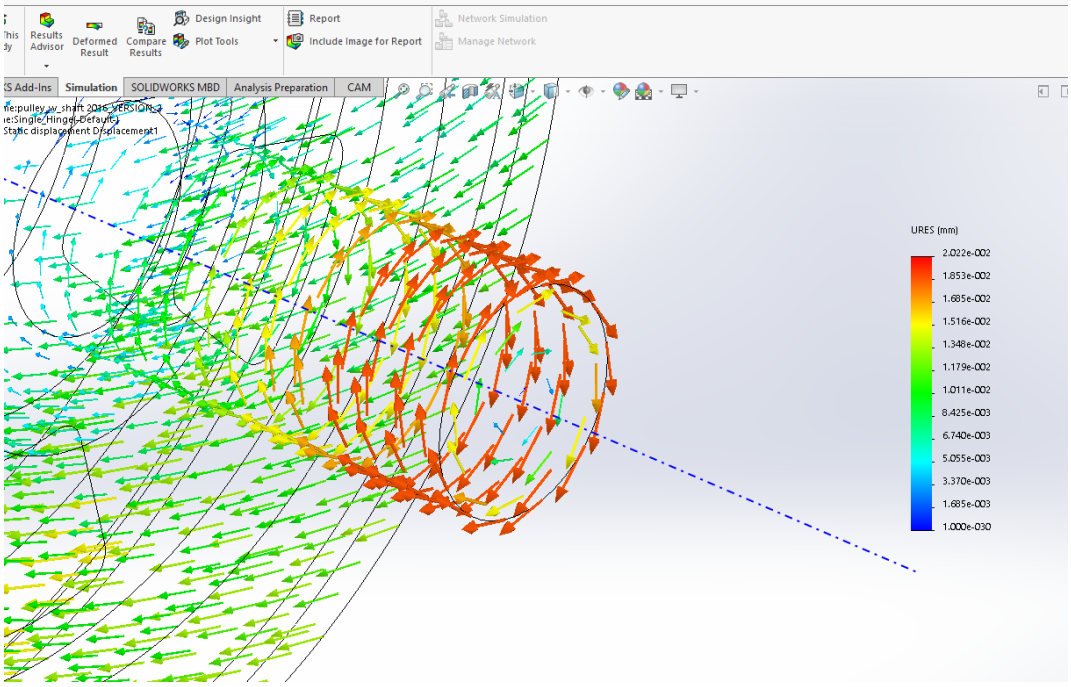

Figure 16: Showing Displacement (As Undeformed Result) Vector Plot of Hinged Portion of Shaft

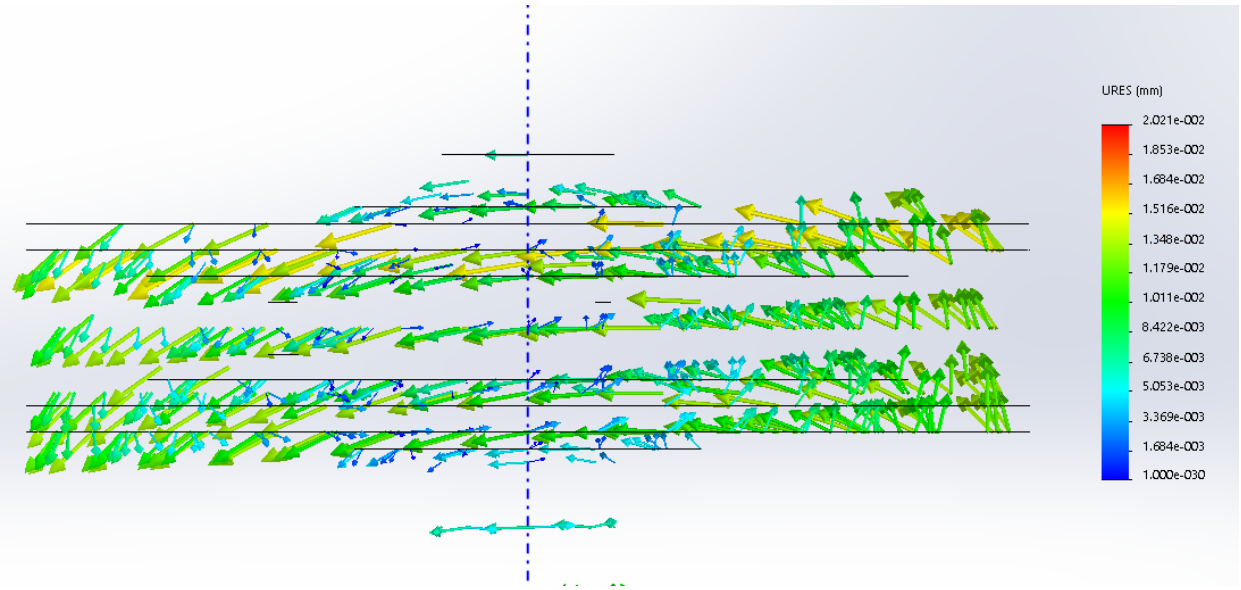

Figure 17: Showing Displacement (As Undeformed Result) Vector Plot of Pulley

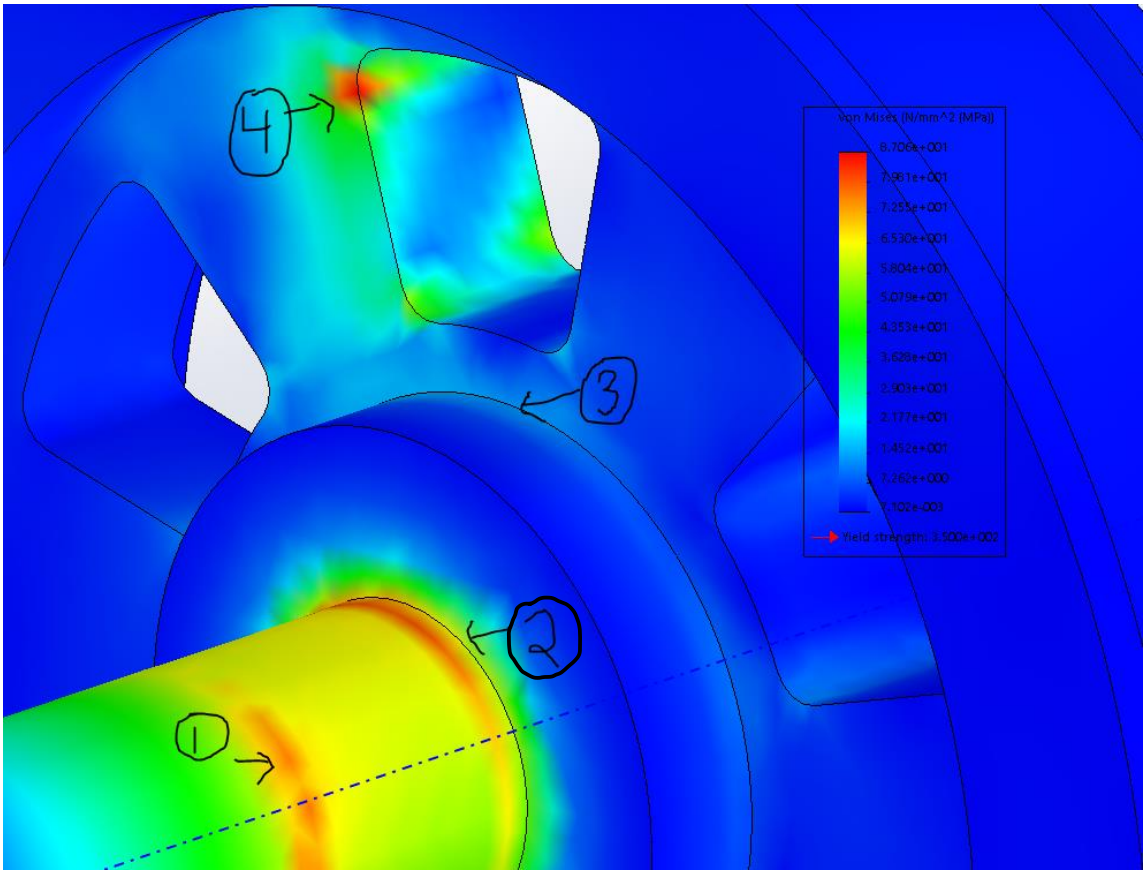

Figure 18: Stress Results for a 2nd Order Global Element Size of 4.00 mm; Each Arrow Points a Region of a Potential Stress Hot Spot

Mesh Type	Mesh Quality	Global Element Size (mm)	Local Element Size (mm)	Ratio	# of Nodes	# of Elements	# of DOF's	Maximum Stress (MPa)	Location of Maximum Stress
Standard	2nd Order	4.00	**2.00**	1.50	63814	41228	191199	**84.632**	Hinge-Unhinged Shaft Interface
"	"	"	**1.00**	"	67959	43983	203634	**105.47**	"
"	"	"	**0.50**	"	75640	49035	226677	**142.21**	"
"	"	"	**0.25**	"	91812	59666	275193	**195.35**	"
"	"	"	**0.125**	"	125646	81953	376695	**273.79**	"

Table 1: Experiment 2—Local h-refinement at **Hinge-Unhinge Interface** (which was a circular edge between the hinged and unhinged portions on the Shaft). Note that the value for stress in this region diverges.

Mesh Type	Mesh Quality	Global Element Size (mm)	Local Element Size (mm)	Ratio	# of Nodes	# of Elements	# of DOF's	Maximum Stress (MPa)	Location of Maximum Stress
Standard	2nd Order	4.00	**2.00**	1.50	71652	46755	214713	**86.56**	Shaft-Disk Interface
"	"	"	**1.00**	"	83660	55449	250737	**108.3**	"
"	"	"	**0.50**	"	108927	73645	326538	**145.7**	"
"	"	"	**0.25**	"	136165	92555	408252	**166.9**	"
"	"	"	**0.125**	"	238162	165978	714243	**222.4**	"

Table 2: Experiment 2—Local h-refinement at **Shaft-Disk** interface. Note that the value for stress in this region also diverges.

Mesh Type	Mesh Quality	Global Element Size (mm)	Local Element Size (mm)	Ratio	# of Nodes	# of Elements	# of DOF's	Maximum Stress (MPa)	Location of Maximum Stress
Standard	2nd Order	4.00	**2.00**	1.50	69612	45138	208593	**17.468**	Disk-Wheel Interface
"	"	"	**1.00**	"	79767	52124	239058	**22.927**	"
"	"	"	**0.50**	"	136175	93031	408282	**30.031**	"
"	"	"	**0.25**	"	174957	119075	524628	**38.82**	"
"	"	"	**0.125**	"	265417	181216	796008	**48.284**	"

Table 3: Experiment 2—Local h-refinement at **Disk-Wheel** interface. Note that the value for stress in this region also diverges.

Mesh Type	Mesh Quality	Global Element Size (mm)	Local Element Size (mm)	Ratio	# of Nodes	# of Elements	# of DOF's	Maximum Stress (MPa)	Location of Maximum Stress
Standard	2nd Order	4.00	**2.00**	1.50	64974	41881	194157	**97.895**	Edge of Fixed Surface
"	"	"	**1.00**	"	74819	48101	221916	**145.23**	"
"	"	"	**0.50**	"	120723	78112	351720	**284.57**	"
"	"	"	**0.25**	"	260737	167299	741174	**326.32**	"
"	"	"	**0.125**	"	843088	544055	2366571	**554.25**	"

Table 4: Experiment 2—Local h-refinement on the **fixed and filleted surfaces** of the hole. Note that the value for stress in this region also diverges.

EXPERIMENT 3 RESULTS:

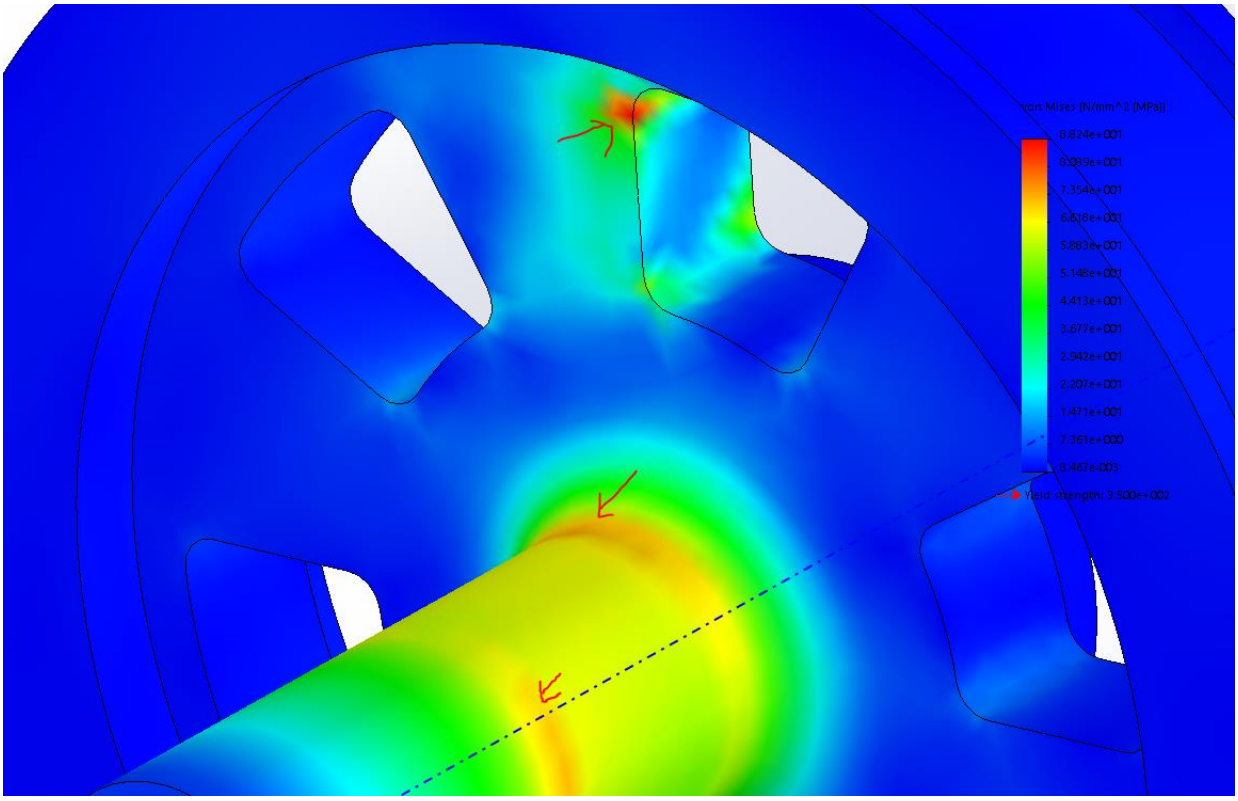

Figure 19: Stress Distribution with Filleted Geometry using 2nd Order, Global Element Size of 4.00 mm

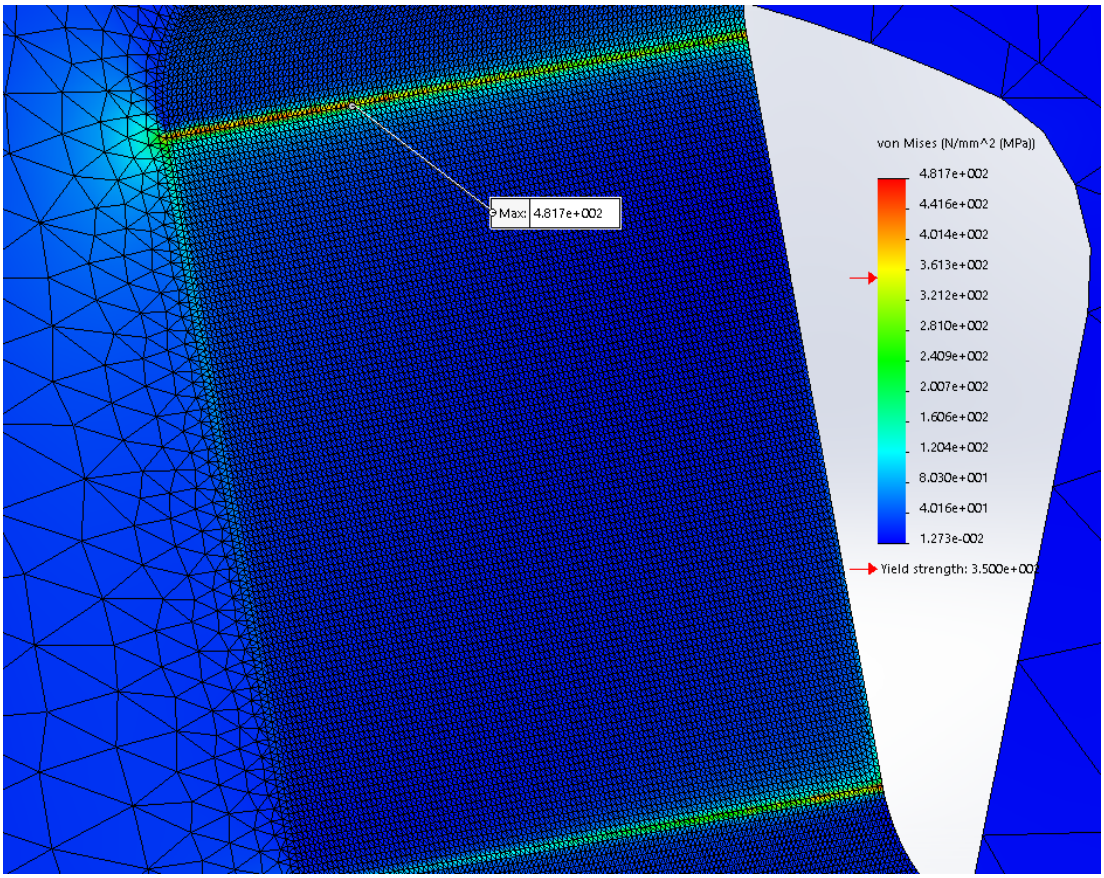

Figure 20: Stress Distribution over Elements on Fixed, Rectangular Surface During an Iteration of local h-refinement

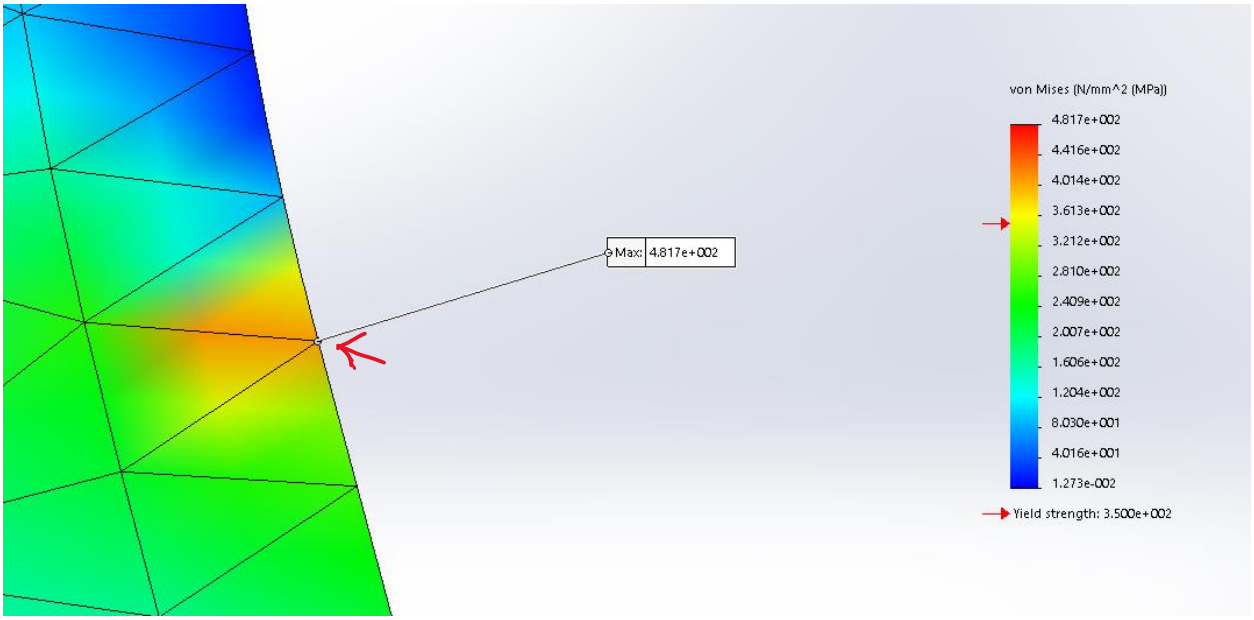

Figure 21: Sharp Turn in Geometry at the Interface between an Element on the Fillet and an Element on the Fixed Rectangular Surface

Mesh Type	Mesh Quality	Global Element Size (mm)	Local Element Size (mm)	Ratio	# of Nodes	# of Elements	# of DOF's	Maximum Stress (MPa)	Location of Maximum Stress
Standard	2nd Order	4.00	**2.00**	1.50	60537	38845	180846	**99.101**	Edge of Fixed Surface
"	"	"	**1.00**	"	65825	42257	194934	**157.75**	"
"	"	"	**0.50**	"	84583	54291	243300	**252.51**	"
"	"	"	**0.25**	"	163539	106363	449580	**403.79**	"
"	"	"	**0.125**	"	434974	283379	1142229	**481.72**	"

Table 5: Experiment 3—Local h-refinement on the **fixed surface**. Note that the value for stress in this region also diverges.

Mesh Type	Mesh Quality	Global Element Size (mm)	Local Element Size (mm)	Ratio	# of Nodes	# of Elements	# of DOF's	Maximum Stress (MPa)	Location of Maximum Stress
Standard	2nd Order	4.00	**2.00**	1.50	71775	46973	215082	**75.216**	Fillet
"	"	"	**1.00**	"	109546	73634	328395	**76.469**	"
"	"	"	**0.50**	"	229824	157733	689229	**75.985**	"
"	"	"	**0.33**	"	401063	276469	1202946	**75.958**	
"	"	"	**0.25**	"	580989	398992	1742724	**75.975**	"

Table 6: Experiment 3—Local h-refinement on the **7.5 mm fillet**. Note that the value for stress in this region finally converges in this region.

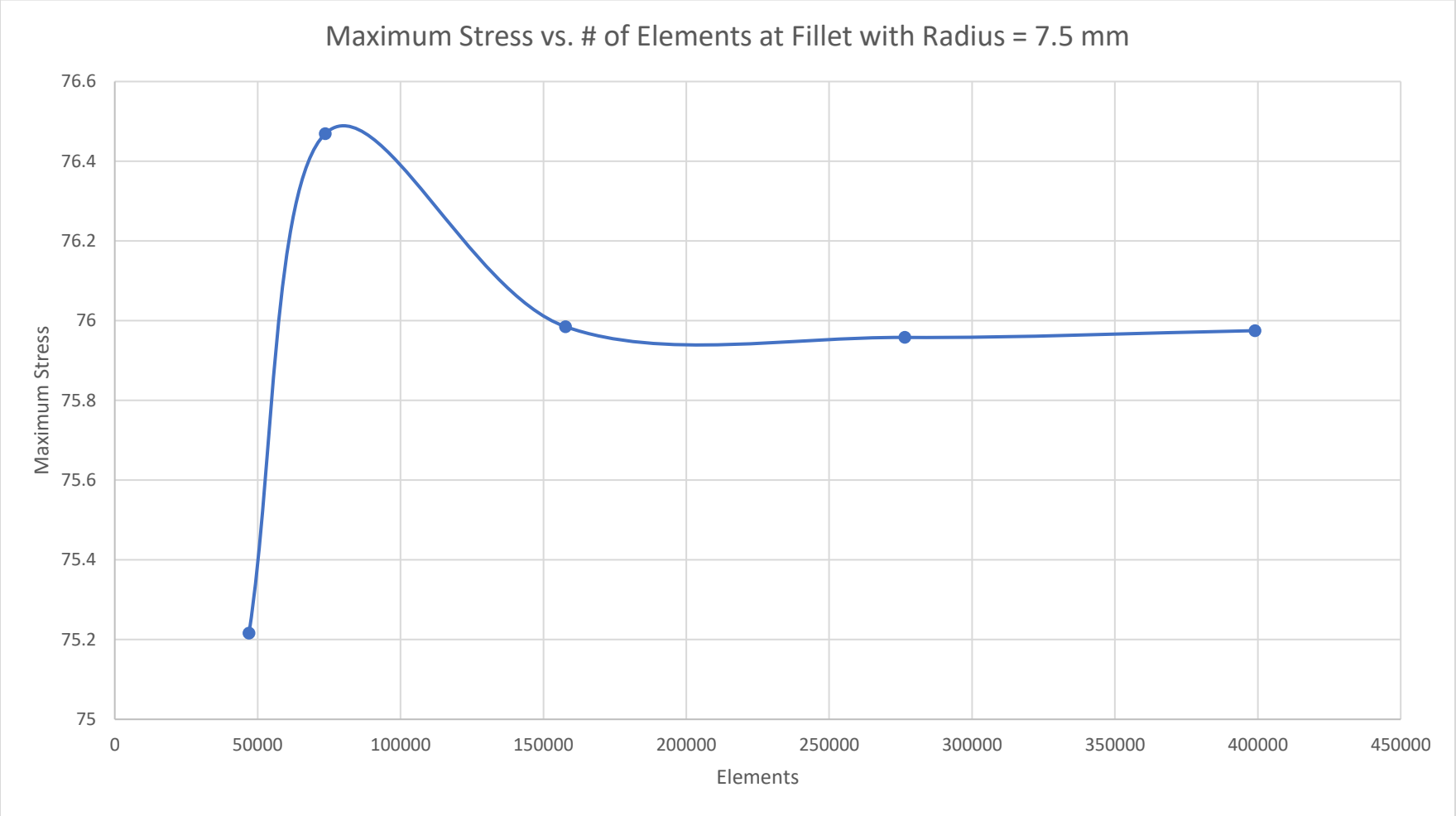

Figure 22: Convergence Plot of Maximum Stress at the Fillet Versus Number of Elements

Discussion

There were a lot of components to this project that I had learned, which I will try to summarize. At the beginning of the project, I used the boundary conditions that were initially suggested to use as a simulation experiment. However, after running the simulation, I realized that the entire shaft and pulley mechanism translated away from its original position. As a result, I knew that these boundary conditions were wrong, and that new boundary conditions had to be applied to the model.

As a result, I began to really study a motor, shaft, and pulley mechanism. I saw that a portion of the shaft that was lodged inside the hub of the motor had to be have as a fixed hinge that had zero degrees of translational freedom and only 1 degree of rotational freedom about its axially symmetric axis. Additionally, I saw that the rest of unhinged portion of the shaft had no restraints on it. I also inspected on the type of restraints the pulley would have by the belt that wraps around it. I initially saw that the tension of the belt could prevent the pulley from translating, but I then pondered on the variance in the type of material used for the belt. As a result, I thought it would be safer to assume that the belt is made from much weaker material than that of steel and that it would be better not to assume that the belt will prevent translational motion on the pulley. Thus, I decided to not put any external restraints on the pulley itself, and that the only restraints applied on the entire model would be the fixed hinge portion of the shaft and the fixed, rectangular surface in one of the holes of the pulley. Finally, I also decided to change the way that torque should be applied on the shaft. By analyzing how a motor should work, I believed that torque should be applied throughout the entire hinged portion of the shaft and not just at the front face of the shaft. I did assume, however, that the entire hinged portion was in direct contact with the motor that is applying torque to the shaft. Thus, I used these boundary conditions for the rest of my simulation studies.

Before running a simulation, I predicted the deformed result using the restraints that I had mentioned previously. I did a static analysis by hand to predict what would happen during the simulation. After running the simulation and looking at the displacement vectors' direction and magnitude, I believed that my prediction was right and that the model should almost behave the way it should in real life.

I then explored possible locations of maximum stress in Experiment 2 by identifying 4 regions of stress hot spots. Two of them were on the shaft-disk and disk-wheel interface. After conducting h-refinement on each of them, the stresses at each location diverged, which was expected because there was a sharp turn in geometry. I knew this could easily be mitigated by applying fillets at each location, but I thought it would be more fruitful to just add 1 fillet that directly connects the shaft to the wheel. I also conducted h-refinement at the hinged-unhinged interface and saw that a stress discontinuity also developed at this location. However, because a sharp turn in geometry develops in this location, it was expected that a stress singularity would occur at this boundary condition. As a result, I decided that it was okay to ignore stress at this location.

I also saw that there was a stress singularity at one of the edges of the fixed, rectangular surfaces of the model during Experiment 2 after conducing local h-refinement. However, I did not want to ignore this stress singularity until after I made the modification to the geometry of the model in Experiment 3, where I added a filleted radius of 7.50 mm, and see if this stress singularity still existed on the modified model.

After making modifications to the original geometry in Experiment 3 by adding a 7.50 mm fillet, there was still a stress concentration at the interface between the hinged and unhinged sections of the shaft, which was expected because I did not change the boundary condition. As a result, the stress at this location was ignored for Experiment 3 as well.

However, stress was still concentrated at the edge of the fixed, rectangular surface in Experiment 3, and I wondered why a stress discontinuity existed at the edge of the fixed surface even thought a fillet existed at this interface. By analyzing the mesh, I saw that despite creating the fillet, the mesh still created a sharp turn in geometry between the fixed faced and filleted surface, and a stress singularity developed as I conducted h-refinement within this region. Thus, I finally believed that the stress in this location can also be ignored during this analysis.

Finally, during Experiment 3, I conducted h-refinement on the revolved, filleted section that directly connected the shaft to the pulley and determined the stress in this location converges to approximately 76 MPa, which was great because this was well beneath the value of 175 MPa.

Final Reflections (Evaluation of Design and What I Would've Done Differently):

The modified model used in Experiment 3, where a fillet was added to connect the shaft directly to the wheel, gave a converged, maximum von Mises stress value of 76 MPa. Because the material used throughout the entire model was made from 1020 cold rolled steel (a ductile material), I used von Mises's definition of stress. Furthermore, I used his failure theory that the maximum von Mises stress should be less than a faction of the maximum yield strength of the material. This fraction is dependent on the size of the factor of safety. Because I wanted a safety factor of 2 and that the yield strength of steel is 350 MPa, the converged, maximum von Mises yield strength during the simulation study should be no larger than 175 MPa.

During Experiment 3, the maximum, converged von Mises stress during the final simulation study was 76 MPa (which was located at the filleted geometry); this value was lower than 175 MPa. Thus, I believe that this model is mostly likely valid and will most likely not fail, if most of my assumptions (boundary conditions of torque and fixed hinges/surfaces) that I've made during the analysis are as closely related as what could occur in real life.

Nonetheless and looking back at the project, I really wished I had more time to do a sensitivity test to more accurately validate my FEM model. I spent most of my time trying to make sure that the boundary conditions made sense because if they didn't, then this problem would cascade throughout my stress analysis of the solution. This was why I did a hand-drawn static analysis to predict what would happen using the boundary conditions I've use for this project, and then tested to see if my predictions were correct after running the simulation. Additionally, I spent a lot of my time exploring the several stress hot spots that I was observed after running the simulation, two of which seemed as an anomaly to me. In fact, two out of the four stress hot spots occurred at the boundary conditions and I did not want to simply ignore these stress concentrations until I understood why they were discontinuous. After understanding why, I then became definitive about why they should also be ignored during the finite element analysis, and then focused on the other stress hotspots instead.

To conduct a sensitivity test, I would create a model with a larger filleted radius. If the maximum stress in this region is lower than 76 MPa, then my assumptions about the boundary conditions of the model would be more valid because having a larger radius would more evenly distribute the stress, unlike a corner that creates a stress discontinuity.